Classical state sensitivity from quantum mechanics

L. E. Ballentine and J. P. Zibin

Physics Department, Simon Fraser University, Burnaby, British Columbia, Canada, V5A 1S6

Sensitivity of the time evolution to small changes in the state is a characteristic feature of classical chaos. It has been believed that state sensitivity could not exist in quantum mechanics because of the unitary invariance of the Hilbert-space overlap of states. We argue that this Hilbert-space criterion is irrelevant and show that both quantum states and classical statistical states exhibit a similar kind of state sensitivity. This is demonstrated by the degree to which the initial state can be recovered in computational motion reversal: forward evolution for a time T, perturbation of the state, and backward time evolution. Some differences between classical and quantum state sensitivity remain, and these seem to be insensitive to decoherence. [S1050-2947(96)06911-9]

I. INTRODUCTION

Understanding the emergence of classical properties from quantum mechanics is a problem as old as quantum theory itself, yet there still remain aspects of it that are not fully understood. The problem is of considerable interest today because of the growing interest in mesoscopic systems [1], whose size places them near the interface between the classical and quantum domains. Perhaps the strongest impetus to study the quantum-classical interface is provided by the phenomenon of *chaos*, which is common in classical mechanics, but very difficult to obtain from quantum mechanics. Chaos in classical mechanics is usually defined as extreme sensitivity to the initial state. Two chaotic orbits that are initially very close together in phase space will separate exponentially with time. After a moderate amount of time has elapsed, the two chaotic orbits may bear no apparent relation to each other.

There is a simple argument that such state sensitivity cannot exist in quantum mechanics. Let $|\psi_1(0)\rangle$ and $|\psi_2(0)\rangle$ be two initial state vectors that differ only slightly, that is,

$$|\langle \psi_1(0)|\psi_2(0)\rangle|^2 = 1 - \epsilon, \qquad (1)$$

with ϵ being a small positive number. It follows from the unitary nature of time development that

$$|\langle \psi_1(t)|\psi_2(t)\rangle|^2 = 1 - \epsilon \qquad (2)$$

for all future times t. Not only do the states not diverge exponentially, but they do not separate at all! This argument is sometimes invoked to prove that there is no chaos in quantum mechanics. But, if taken at face value, it would prove not only that chaos is absent in quantum mechanics, but that chaos cannot even emerge asymptotically in the classical limit. While the former conclusion may be acceptable, the latter conclusion is very alarming, for it would mean that classical mechanics cannot be obtained as a limit of quantum mechanics.

That this radical conclusion is unjustified is strongly indicated by the fact that a parallel argument can be given for the nonexistence of *classical* chaos. It is based on the statistical form of classical mechanics and the Liouville equation for the phase space distribution function,

$$\frac{\partial}{\partial t}\rho(q,p,t) = -\frac{p}{m}\frac{\partial}{\partial q}\rho(q,p,t) - F(q)\frac{\partial}{\partial p}\rho(q,p,t). \qquad (3)$$

Here, q and p denote the position and momentum, and $F(q)$ is the external force exerted on the system. Let $\rho_1(q,p,0)$ and $\rho_2(q,p,0)$ be two initial phase-space distributions that are close, in the sense that their overlap is almost total. That is, we have (for a suitable choice of normalization)

$$\int \int \rho_1(q,p,t)\rho_2(q,p,t)dq \; dp = 1 - \epsilon \qquad (4)$$

at $t=0$. But Liouville's theorem proves that this overlap integral is independent of t; therefore, initially close classical (statistical) states do not separate in time. So if Eq. (2) really proved the absence of quantum chaos, then Eq. (4) would equally prove the absence of classical chaos. But the conclusion of this argument is, of course, false.

The problem with the above argument is not mathematical, but conceptual. There are two senses of the word *state* in classical mechanics: the individual state (orbit) and the statistical state (phase-space probability distribution). In quantum mechanics, on the other hand, all states (pure or mixed) are subject to a statistical interpretation, and there is no analog of the individual orbit. The usual definition of classical chaos, as an exponentially rapid separation of initially close states, applies only to the individual states. A different criterion must be used to identify chaos in a classical statistical state.

A conceivable (but not practical) method would be to consider two initial phase-space distributions that are sharply peaked, nonoverlapping, and separated by a very small distance. If the motion is chaotic, then the separation between the centers of these two distributions will initially grow exponentially (and, of course, the peaks will broaden). But the Hilbert-space separation of the two distribution functions, as measured by their overlap integral [Eq. (4)], will remain constant. This overlap has the same value (zero), regardless of whether the distance between the peaks is a millimeter or a mile. Thus we see that the Hilbert-space overlap, as a measure of the ''closeness'' of two classical distribution func-

tions, is entirely irrelevant to the existence or nonexistence of chaos in a classical system.

A quantum state is more analogous to a classical statistical state than to a single classical orbit [2], and the similarity between Eqs. (2) and (4) strongly suggests that the constancy of the Hilbert-space overlap is just as irrelevant to the existence or nonexistence of chaos in quantum mechanics as it is in classical mechanics. Quantum chaos, defined as the analog of classical chaos, should, therefore, be sought by comparing quantum phenomena with the manifestations of chaos in the classical Liouville equation.

Two kinds of sensitivities can be distinguished in dynamics: (i) sensitivity of the motion to small changes in the Hamiltonian, and (ii) sensitivity to small changes in the state, with the Hamiltonian being unchanged. Both of these can be regarded as modeling the effect of an external perturbation. If the ''environment,'' which is the source of the perturbation, were described by a Hamiltonian and included within the system, then cases (i) and (ii) could be treated within a unified framework. But that is frequently impractical, and as long as the perturbation is regarded as external to the system, the two cases remain formally distinct.

Peres [3,4] has made a thorough study of case (i). He finds that quantum motions are much more sensitive to a small perturbation of the Hamiltonian, δH, if the underlying classical motion is chaotic than if it is regular. This sensitivity can be measured in various ways. One criterion [4] is the decay of the overlap between the time-dependent states $|\psi(t)\rangle$ and $|\psi'(t)\rangle$, where $|\psi(0)\rangle = |\psi'(0)\rangle$, but $|\psi(t)\rangle$ evolves under H while $|\psi'(t)\rangle$ evolves under $H + \delta H$. Another [4,5] is the degree of mixing of the eigenstates of $H + \delta H$ when expressed in terms of the eigenstates of H. As a result of these investigations, the sensitivity of quantum motions to perturbations of the Hamiltonian is reasonably well understood.

But this does not provide an understanding of how the sensitivity of classical motions to small changes in the state can arise from quantum mechanics. We argue that such an understanding can come only by comparing quantum phenomena with the manifestations of chaos in the classical Liouville equation. Such a strategy has been applied to the quantum baker's map [6], using an analysis of the information needed to track the state in detail. The results show a similar sensitivity to perturbations in both the classical and quantum maps. Unfortunately, it is difficult to apply that method to real dynamical systems that satisfy Liouville's equation or Schrödinger's equation.

In this paper we use computational motion reversal—the accuracy with which a time-reversed system returns to its initial state—as a measure of state sensitivity. Our results show that, by this criterion, quantum systems exhibit a form of state sensitivity very similar to that of classical systems.

II. MOTION REVERSAL

The technique of computational motion reversal was first used to illustrate the difference between the stabilities of classical and quantum dynamics. In this method, a state is propagated from time $t=0$ to $t=T$, subjected to motion reversal at $t=T$, and then propagated until $t=2T$. Because the dynamics are theoretically reversible, the initial state should be recovered. When this was done for two systems that exhibit diffusive motion (in momentum space), the kicked rotator [7] and a hydrogen atom in a microwave radiation field [8], it was found that the quantum dynamics was indeed reversible to within expected numerical accuracy. For $t>T$, the classical system initially began to retrace its motion, but it soon returned to diffusive motion and did not even approximately recover its initial state. This was caused by the inevitable truncation and roundoff errors, which grow exponentially (at a rate governed by the largest Lyapunov exponent) in the classical case, but do not grow exponentially in the quantum case.

Those calculations provide a spectacular demonstration of the ''practical irreversibility'' of classical mechanics, as compared with quantum mechanics. But they are less satisfactory as a true measure of the degree of state sensitivity in the two theories. The ''perturbations'' to which the states are subjected, roundoff and truncation errors, are machine dependent and uncontrolled. They correspond to no physical phenomenon. There is no assurance that the quantum and classical states are equivalently perturbed, since they are represented mathematically, and hence computationally, in such different ways. What is really being compared is the stability of two different computational algorithms, rather than two physical processes.

To overcome these limitations, we have modified the procedure thus: the state is propagated from $t=0$ to $t=T$; a perturbation of controlled magnitude (large compared to the roundoff error) is applied; and the motion-reversed state is propagated from $t=T$ to $t=2T$. The accuracy with which the initial state is recovered can then be studied as a function of the magnitude of the perturbation and the duration T of propagation. The simplest perturbation is a spatial displacement of length δq, which can obviously be applied equally to a quantum or a classical state.

For quantum mechanics, the probability of return to the initial state $|\psi(0)\rangle$ is given by

$$S_{\text{qm}}(\delta q, T) = |\langle \psi(0) | U(-T) D(\delta q) U(T) | \psi(0) \rangle|^2, \quad (5)$$

where $U(T)$ is the time-development operator and $D(\delta q)$ is the displacement operator. Because the time-development operator is unitary, this is equivalent to

$$S_{\text{qm}}(\delta q, T) = |\langle \psi(T) | D(\delta q) | \psi(T) \rangle|^2$$

$$= \left| \int \psi^*(q, T) \psi(q - \delta q, T) dq \right|^2, \quad (6)$$

where $|\psi(T)\rangle = U(T)|\psi(0)\rangle$, and $\psi(q, T) = \langle q | \psi(T) \rangle$ is the wave function in coordinate representation. So we need not integrate the equation of motion from T to $2T$; it suffices to integrate only from 0 to T, and to calculate the overlap between $|\psi(T)\rangle$ and the displaced state $D(\delta q)|\psi(T)\rangle$.

Similarly, for classical mechanics, we define the overlap between initial and final phase-space distributions,

$$S_{\text{cl}}(\delta q, T) = N \int \int \rho(q, p, 0) U_L(-T)$$

$$\times D_L(\delta q) U_L(T) \rho(q, p, 0) dq \, dp, \quad (7)$$

where $U_L(T)$ and $D_L(\delta q)$ are the time-development and space-displacement operators for the Liouville distribution.

The normalization constant N is chosen so that $S_{cl}(0,T) = 1$. Liouville's theorem guarantees that the overlap between two phase-space distributions is constant in time, so Eq. (7) is equivalent to

$$S_{cl}(\delta q, T) = N \int \int \rho(q,p,T)\rho(q-\delta q, p, T)dq \ dp. \quad (8)$$

The accumulation of roundoff errors, though unavoidable, plays no relevant role in our results because we integrate the equation of motion only from $t=0$ to $t=T$ and do not need to perform a compensating motion-reversed integration from T to $2T$.

That the appropriate quantum analog of Eq. (8) is Eq. (6), with the square of the inner product rather than some other power, can be justified by means of the Wigner function,

$$\rho_w(q,p,t) = (2\pi\hbar)^{-1} \int e^{ipx/\hbar} \langle q - x/2|\psi\rangle\langle\psi|q+x/2\rangle dx. \quad (9)$$

In the Wigner representation, Eq. (6) becomes

$$S_{qm}(\delta q, T) = 2\pi\hbar \int \int \rho_w(q,p,T)\rho_w(q-\delta q, p, T)dq \ dp. \quad (10)$$

The Wigner function is not a probability distribution, since it can be negative, and it need not even possess a classical limit. But in those special cases where it is positive and does have a classical limit, it satisfies the Liouville equation (3) in that limit. This reassures us that $S_{qm}(\delta q, T)$ and $S_{cl}(\delta q, T)$ are appropriate quantities for comparison. By studying the overlap between perturbed and unperturbed states, we are using a criterion similar to that used by Peres [4] to study the effects of perturbations in the Hamiltonian. This may facilitate comparison between the cases of state perturbations and of Hamiltonian perturbations.

III. THE MODELS

Two models have been studied, the driven quartic oscillator and the periodically kicked rotator.

(a) The Hamiltonian of the *driven quartic oscillator* is

$$H = p^2/2M + bq^4 - aq \ \cos(\omega t). \quad (11)$$

The solution of Liouville's equation is equivalent to the solution of Hamilton's equations for an ensemble of particles, and this method of simulation is often a more effective computational technique than a direct solution of Liouville's differential equation. The classical equations of motion were integrated by an Adams-method ordinary-differential-equation (ODE) integrator. The quantum Hamiltonian is obtained by replacing the momentum variable with $p = -i\hbar\partial/\partial q$, whence the Schrödinger equation, $H\psi(q,t) = i\hbar\partial\psi/\partial t$, becomes a partial differential equation in q and t. A finite difference approximation for the q dependence reduces this to a large set of coupled ordinary differential equations, which were solved by a Runge-Kutta-Merson ODE integrator.

The classical parameter values used were $M=1$, $b=0.25$, $a=0.5$, and $\omega=1$. For these values, it has previously been

shown (see Fig. 1 of [9]) that the Poincaré section of the classical orbits contains a large regular island surrounded by a larger chaotic zone. The smallest value of $\hbar$ that we found to be computationally practical was 0.02. In these units, the area of the regular island is 2.25, which can support $2.25/2\pi\hbar = 17.9$ quantum states; the combined area of the regular island and the surrounding chaotic zone is 10.1, which can support $10.1/2\pi\hbar = 80.4$ quantum states.

(b) The Hamiltonian of the *periodically kicked rotator* is

$$H = \frac{p^2}{2I} + C \ \cos\theta \sum_{n=1}^{\infty} \ \delta(n - t/\tau). \quad (12)$$

Here, p is the angular momentum, I is the moment of inertia, τ is the interval between kicks, and $C\tau$ is the maximum angular impulse per kick. If p_n and θ_n denote the values just before the nth kick, then the values just before the $(n+1)$th kick are given by

$$p_{n+1} = p_n + C\tau \ \sin(\theta_n), \quad (13)$$

$$\theta_{n+1} = \theta_n + (\tau/I)p_{n+1}. \quad (14)$$

In terms of the dimensionless variables $y = (\tau/2\pi I)p$ and $x = \theta/2\pi$, these equations reduce to the so-called *standard map* [10],

$$y_{n+1} = y_n + (K/2\pi)\sin(2\pi x_n), \quad (15)$$

$$x_{n+1} = x_n + y_{n+1}, \quad (16)$$

where $K = C\tau^2/I$ is the dimensionless kick-strength parameter.

The quantum Hamiltonian is obtained by replacing the momentum variable by $p = -i\hbar \partial/\partial\theta$. The time-development operator that takes the state vector through the nth kick to just before the $(n+1)$th kick is

$$U(\tau) = \exp\{-ip^2\tau/2I\hbar\}\exp\{-iC\tau \ \cos(\theta)/\hbar\}. \quad (17)$$

The rightmost factor in Eq. (17), which describes the kick, is easy to apply in coordinate representation. The leftmost factor, which describes the free rotation between kicks, is easy to apply in momentum representation, where its matrix representation is $\langle m|\exp(-ip^2\tau/2I\hbar)|m'\rangle = \exp(-im^2\hbar\tau/2I)\delta_{m,m'}$. ($\hbar m$ is an eigenvalue of p.) Therefore, the time integration of the Schrödinger equation is performed thus: choose an initial state vector in coordinate representation; multiply by $\exp(-i\beta \cos\theta)$; fast-Fourier-transform (FFT) to the momentum representation; multiply by $\exp(-i\alpha m^2/2)$; FFT to the coordinate representation; etc. The two dimensionless parameters are

$$\alpha = \hbar\tau/I \quad \text{and} \quad \beta = C\tau/\hbar. \quad (18)$$

Their product is the classical kick strength $K = \alpha\beta = C\tau^2/I$.

The initial quantum state $|\psi(0)\rangle$ is chosen to be a localized wave packet. The corresponding classical distribution is constructed to have the same initial position and momentum distributions,

$$\rho(q,p,0) = |\langle q|\psi(0)\rangle|^2|\langle p|\psi(0)\rangle|^2. \quad (19)$$
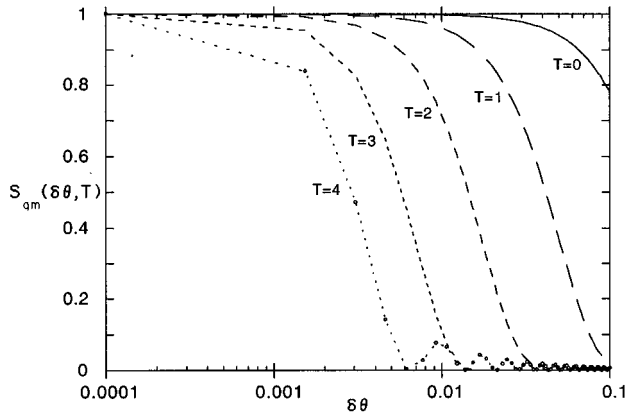
FIG. 1. Overlap function for the quantum kicked rotator ($K = 0.97$, $\alpha = 0.005$). T is the number of kicks before the displacement $\delta\theta$ is applied.

The manner in which differences between the classical and quantum probabilities develop and grow with time was studied in a previous publication [2].

IV. RESULTS

Figure 1 shows the overlap function for displaced quantum states [Eq. (6)] of the kicked rotator, for various propagation times. (For the rotator, the displacement δq is the angle $\delta\theta$.) For $T = 0$, the decrease of $S_{qm}(\delta q, T)$ with increasing δq merely reflects the width of the initial wave packet. As T increases, the state develops more complex fine structure and becomes more sensitive to displacements. Hence, for fixed δq, $S_{qm}(\delta q, T)$ initially decreases as T increases, and for fixed T, $S_{qm}(\delta q, T)$ decreases as δq increases.

Since the (classical or quantum) overlap $S(\delta q, T)$ drops from a value near one to a value near zero within a small range of δq, it is convenient to characterize the state by the value $\delta q_{1/2}(T)$ for which the overlap falls to one-half,

$$S(\delta q_{1/2}, T) = \tfrac{1}{2}. \qquad (20)$$

This quantity $\delta q_{1/2}$ ($\delta\theta_{1/2}$ for the rotator) is a convenient measure of the *robustness* of the state, by which we mean its ability to sustain a perturbation and yet return after motion reversal to approximately the initial state.

Some results for the driven quartic oscillator are shown in Figs. 2 and 3. A quantum wave-packet state with standard deviations $\Delta q = \Delta p = 0.1$ was placed at $\langle q \rangle = \langle p \rangle = 1$, which is within the regular island of phase space (see Fig. 1 of [9]), and a similar classical ensemble [Eq. (19)] was also propagated. We see (Fig. 2) that the perturbation sensitivity of the nonchaotic state changes only very slowly with propagation time, and also that the sensitivities displayed by the classical and quantum systems are very similar over the range of times studied.

A similar quantum wave packet and classical ensemble were placed at $\langle q \rangle = 0.2$, $\langle p \rangle = 0$, which is in the chaotic zone, and the results (Fig. 3) are quite different. The robustness of the classical state decreases rapidly with propagation time. The robustness of the quantum state initially falls with its classical analog, but after a certain time it reaches a pla-
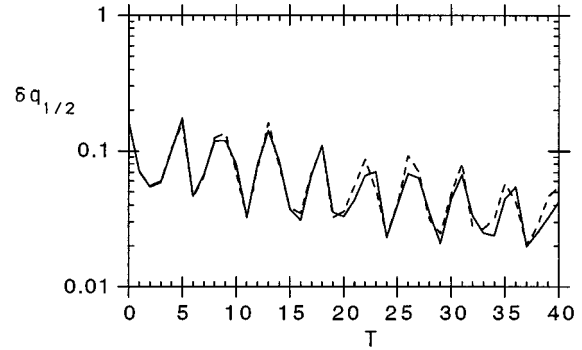
FIG. 2. Robustness parameter $\delta q_{1/2}(T)$ for a nonchaotic state of the driven anharmonic oscillator. T is in units of the driving force period. Solid line: classical state. Dashed line: quantum state with $\hbar = 0.02$.

teau. No matter how long the propagation time T, there is a minimum perturbation δq required to prevent the quantum state from recurring after motion reversal. This minimum δq is roughly equal to the smallest de Broglie wavelength that plays a significant role in the state. This argument can be made more precise by writing Eq. (6) as

$$S_{qm}(\delta q, T) = \left| \int |\psi(p, T)|^2 e^{-ip\,\delta q/\hbar} dp \right|^2, \qquad (21)$$

where $\psi(p, T) = \langle p | \psi(T) \rangle$ is the momentum wave function. Thus $S_{qm}(\delta q, T)$ is the square of the Fourier transform of the momentum distribution function $|\psi(p, T)|^2$, and its spatial extent will be inversely related to the width of the momentum distribution. Apart from a factor of order unity, we may expect $\delta q_{1/2}(T) \gtrsim \hbar / \Delta p(T)$, with approximate equality holding when $\delta q_{1/2}(T)$ reaches its plateau. The state rapidly spreads to fill the entire chaotic zone, so the limiting value of Δp can be estimated from the size of the chaotic zone, and indeed $\hbar / \Delta p$ provides an estimate for the observed minimum value of $\delta q_{1/2}$. Figure 3 also shows $\delta q_{1/2}$ for
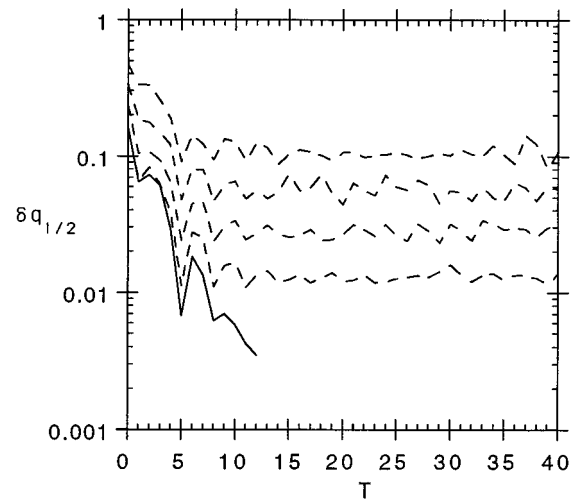
FIG. 3. Robustness parameter $\delta q_{1/2}(T)$ for a chaotic state of the driven anharmonic oscillator. Dashed lines (top to bottom): quantum state ($\hbar = 0.16$, 0.08, 0.04, 0.02). Solid line: classical state with the same initial Δq and Δp as the $\hbar = 0.02$ quantum state.
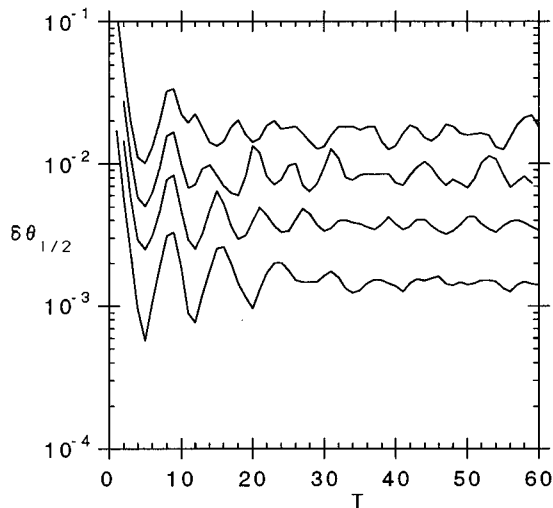
FIG. 4. Robustness parameter $\delta\theta_{1/2}(T)$ for a bounded chaotic state of the quantum kicked rotator ($K=0.97$). From top to bottom, the curves correspond to $\alpha=0.02$, 0.01, 0.005, 0.002. ($\alpha=\hbar\tau/I$.)

FIG. 5. Robustness parameter $\delta\theta_{1/2}(T)$ for an unbounded chaotic state of the quantum kicked rotator ($K=4$; $\alpha=0.02$).

three other values of $\hbar$, confirming that the plateau of $\delta q_{1/2}(T)$ does indeed scale with $\hbar$.

The momentum of the classical kicked rotator is bounded by a Kolmogorov-Arnold-Moser (KAM) surface if the kick strength is less than $K_c=0.9716...$ [10]. Although the quantum system can tunnel through the KAM barrier, this is a very small effect, and the momentum is practically bounded in the quantum system too. Figure 4 shows the robustness parameter $\delta\theta_{1/2}(T)$, calculated for $K=0.97$ and several values of $\alpha=\hbar\tau/I$. These results, like those for the driven oscillator (Fig. 3), show that as T increases, $\delta\theta_{1/2}$ first decreases but then reaches a plateau of order $\hbar/\Delta p$.

For $K>K_c$, the momentum of the classical kicked rotator increases diffusively without bound, and the width of the momentum distribution grows like $t^{1/2}$. In this regime of unbounded motion, the robustness parameter of the quantum system does not plateau. The slope of the log-log plot (Fig. 5) shows that $\delta\theta_{1/2}(T)$ is proportional to $T^{-1/2}$ at large T, as would be expected from the estimate $\hbar/\Delta p(T)$. (The phenomenon of quantum localization [11], which limits the diffusive growth of the momentum, does not occur until times larger that those shown in Fig. 5.)

The classical and quantum systems are compared in Figs. 6 and 7 for two values of $\alpha=\hbar\tau/I$. In both cases, the theories agree initially, but the robustness of the quantum state reaches a plateau as T increases, whereas the robustness of the classical state decreases without bound.

V. DISCUSSION

It has previously been shown [4] that the time evolution of a quantum system is more sensitive to small perturbations in the Hamiltonian if the analogous classical system is chaotic than if it is not chaotic. But sensitivity to small changes in the quantum state, for a fixed Hamiltonian, was believed not to exist because of the unitary invariance of Hilbert-space overlap of states. We have argued that the Hilbert-space overlap criterion is not relevant to the existence of chaos in either quantum or classical mechanics. Instead, we
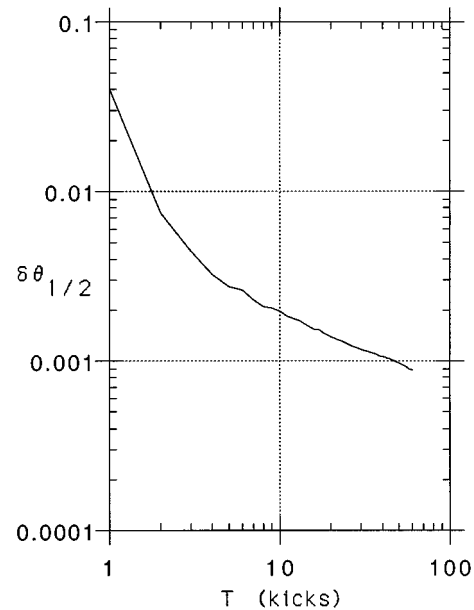
characterize the state sensitivity of a classical or quantum system by a parameter called the *robustness*, which is the largest perturbation that can be applied to the state after propagation for a time T without preventing the system from approximately recovering its initial state after motion reversal. As T increases, an initially smooth state develops finer structures, which are more sensitive to perturbations, and the robustness decreases. The robustness decreases very slowly with time for nonchaotic states, but very rapidly for chaotic states. For short times, the state sensitivities of classical and quantum systems are very similar. For long times, the robustness of a chaotic classical state decreases (roughly exponentially) without bound, but the robustness of the corresponding quantum state decreases much more slowly. We have argued that the minimum perturbation required to prevent a
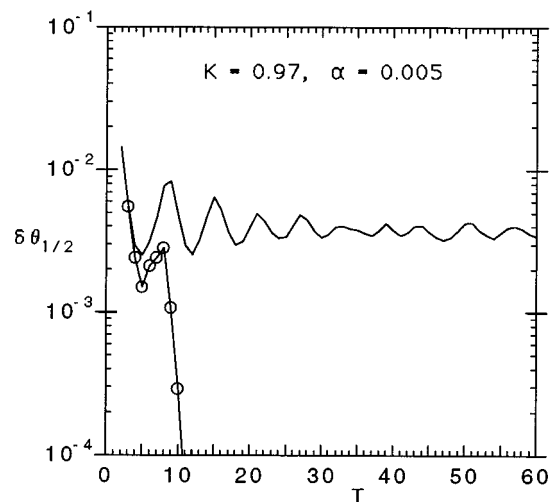
FIG. 6. Robustness parameter $\delta\theta_{1/2}(T)$ for a bounded chaotic state of the classical (circles) and quantum (plain line) kicked rotator ($K=0.97$, $\alpha=\hbar\tau/I=0.005$).

FIG. 7. Robustness parameter $\delta\theta_{1/2}(T)$ for a bounded chaotic state of the classical (circles) and quantum (plain line) kicked rotator ($K=0.97$, $\alpha=\hbar\tau/I=0.01$).

FIG. 8. Example of the extrapolation to obtain one classical point ($T=5$) in Fig. 6. Values were computed on $g \times g$ grids for ensembles of n particles: $n=100\,000$ (circle); $200\,000$ (square); $400\,000$ (diamond); $800\,000$ (triangle). The solid line is the $n \rightarrow \infty$ limit.
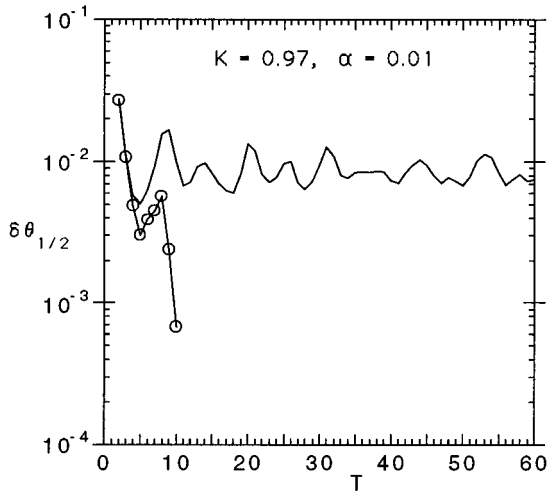
quantum system from returning to its initial state after motion reversal, $\delta q_{1/2}(T)$, is governed by the smallest de Broglie wavelength in the state. Therefore, if the motion is bounded in momentum space, $\delta q_{1/2}(T)$ will plateau at a value of order $\hbar/\Delta p$. If the momentum distribution width Δp is not bounded, then $\delta q_{1/2}(T)$ continues to decrease with T, in inverse proportion to Δp.

The break between the quantum and classical behaviors is very striking for chaotic states (Figs. 3, 6, and 7). One would expect the time of the break to increase as $\hbar$ decreases, so that full quantum-classical correspondence would emerge in the limit $\hbar \rightarrow 0$. This is not seen in our results, and the reason may not be due merely to the limited range of $\hbar$ values that we were able to study. As was stressed in [2], the quantum state depends on $\hbar$, so the limit $\hbar \rightarrow 0$ involves a sequence of states that must be chosen in a physically appropriate manner. In particular, the common choice of Gaussian wave packets with $\Delta q \sim \Delta p \sim \hbar^{1/2}$ is arbitrary and lacks physical significance.

A more appropriate procedure is to hold constant, as $\hbar \rightarrow 0$, the initial probability distributions of macroscopically significant variables. But which distributions need to be controlled? In our calculations, the initial position distribution was held constant, since it is the position distribution that determines the applicability or inapplicability of Ehrenfest's theorem [2]. But in Figs. 6 and 7 it is apparent that the classical results depend on $\hbar$. This occurs because the initial classical ensemble was constructed to have the same position and momentum distributions as the initial quantum state. If Δq is held constant, then Δp will scale with $\hbar$. As time increases, the phase-space distribution develops essentially the same filamentary structure, regardless of the (small) initial Δp, but the thickness of the filaments depends on the initial Δp. This makes no difference to the low-order moments of the distribution (such as were studied in [2]), but it does affect the overlap function. Thus the classical value of $S_{cl}(\delta q,T)$ becomes a "moving target" as $\hbar \rightarrow 0$. In order to see $S_{qm}(\delta q,T)$ converge onto a definite $S_{cl}(\delta q,T)$ as $\hbar \rightarrow 0$, it will be necessary to hold *both* the initial position and momentum distributions constant as $\hbar \rightarrow 0$, so that the corre-

sponding classical ensemble does not vary with $\hbar$. This will require the use of mixed quantum states (density matrices), since a wave packet necessarily has $\Delta p \propto \hbar/\Delta q$. Although feasible, this will be computationally demanding, and has not yet been done. (A 2048×2048 density matrix will take 2048 times as long to compute as a 2048-component state vector.)
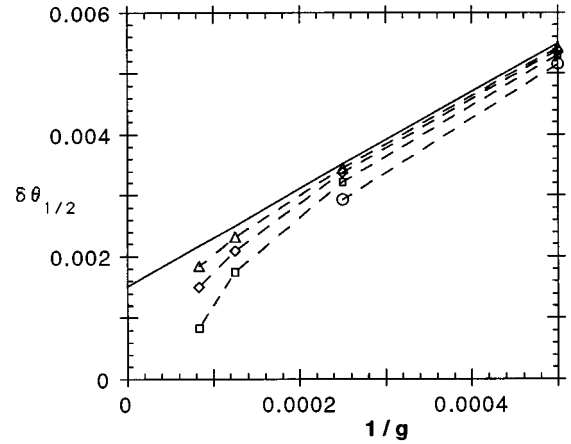
Decoherence (the loss of quantum coherence due to interaction with the environment) is sometimes invoked [12,13] to explain the emergence of classical properties (including chaos) from quantum mechanics. Although decoherence can be effective in eliminating interference patterns, it will not reduce the striking differences between $S_{qm}(\delta q,T)$ and $S_{cl}(\delta q,T)$. The large-T plateau in $S_{qm}(\delta q,T)$ is governed by the minimum de Broglie wavelength, which will not be affected by weak environmental interactions. Thus, although decoherence may be relevant to the study of the quantum-to-classical interface, it is not fully responsible for the emergence of classical behavior.

APPENDIX: COMPUTATION OF CLASSICAL PHASE-SPACE INTEGRALS

The evaluation of $S_{cl}(\delta q,T)$ from Eq. (8) requires the integration of a function of the phase-space density $\rho(q,p,t)$. But $\rho(q,p,t)$ is not available as a continuous function; we have only a finite ensemble of points distributed over phase space. The probability density can be estimated by dividing phase space into a grid of cells and counting the number of points in each cell. One might think that the integral [Eq. (8)] would be accurately estimated if we choose a fine enough grid. But that is not so. As the grid becomes ever finer, the histogram approximation to $\rho(q,p,t)$ approaches a set of delta functions, and the overlap [Eq. (8)] tends to zero. It is

necessary to compute the histogram for an ensemble of n particles on a grid of $g \times g$ cells, for several values of n and g, and perform a double extrapolation. For fixed grid size g, the results vary nearly linearly with $1/n$, and an accurate extrapolation to the infinite n limit is possible. This yields the solid line in Fig. 8, which can then be extrapolated to the continuum limit ($1/g \rightarrow 0$). It is apparent from Fig. 8 that no feasible value of n or g can be considered ''large enough.'' Only by this double-extrapolation method can reliable values be obtained.

---

[1] See, for example, *Quantum Complexity in Mesoscopic Systems*, edited by A. R. Bishop, R. E. Ecke, and R. Mainieri (North-Holland, Amsterdam, 1995).

[2] L. E. Ballentine, Yumin Yang, and J. P. Zibin, Phys. Rev. A **50**, 2854 (1994).

[3] A. Peres, Phys. Rev. A **30**, 1610 (1984).

[4] A. Peres, *Quantum Theory: Concepts and Methods* (Kluwer, Dordrecht, 1993), Chap. 11.

[5] L. Benet, T. H. Seligman, and H. A. Weidenmüller, Phys. Rev. Lett. **71**, 529 (1993).

[6] R. Schack and C. M. Caves, Phys. Rev. Lett. **71**, 525 (1993).

[7] D. L. Shepelyansky, Physica (Amsterdam) **8D**, 208 (1983).

[8] G. Casati, B. V. Chirikov, I. Guarneri, and D. L. Shepelyansky, Phys. Rev. Lett. **56**, 2437 (1986).

[9] N. Ben-Tal, N. Moiseyev, and H. J. Korsch, Phys. Rev. A **46**, 1669 (1992).

[10] A. J. Lichtenberg and M. A. Lieberman, *Regular and Chaotic Dynamics* (Springer, New York, 1992).

[11] D. R. Grempel, R. E. Prange, and S. Fishman, Phys. Rev. A **29**, 1639 (1984).

[12] W. H. Zurek and J. P. Paz, Physica D **83**, 300 (1995).

[13] K. Shiokawa and B. L. Hu, Phys. Rev. E **52**, 2497 (1995).